Available online at www.sciencedirect.com
SCIENCE DIRECT
International Journal of Heat and Mass Transfer 49 (2006) 1833–1844
International Journal of HEAT and MASS TRANSFER
www.elsevier.com/locate/ijhmt

A numerical model for heat sinks with phase change materials and thermal conductivity enhancers

K.C. Nayak, S.K. Saha, K. Srinivasan, P. Dutta *

Department of Mechanical Engineering, Indian Institute of Science, Bangalore 560012, India

Received 23 March 2005
Available online 19 January 2006

Abstract

The effectiveness of thermal conductivity enhancers (TCEs) in improving the overall thermal conductance of phase change materials (PCMs) used in cooling of electronics is investigated numerically. With respect to the distribution of TCE and PCM materials, the heat sink designs are classified into two types. The first type of heat sink has the PCM distributed uniformly in a porous TCE matrix, and the second kind has PCM with fins made of TCE material. A transient finite volume method is used to model the heat transfer; phase change and fluid flow in both cases. A generalized enthalpy based formulation and numerical model are used for simulating phase change processes in the two cases. The performance of heat sinks with various volume fractions of TCE for different configurations is studied with respect to the variation of heat source (or chip) temperature with time; melt fraction and dimensionless temperature difference within the PCM. Results illustrate significant effect of the thermal conductivity enhancer on the performance of heat sinks.

Keywords: Heat sink; Phase change material; Thermal conductivity enhancer; Modeling

1. Introduction

As each new generation of electronic products squeezes more power and performance into ever-small packages, the relative importance of thermal management within the overall product design continues to increase. In recent years, PCMs have been widely used as an alternative cooling method for various applications such as spacecraft and avionics thermal control, personal computing and communication equipment, wearable computers, power electronic equipment, portable phones etc. Passive thermal management scheme of PCMs can be used in situations where heat dissipation is periodic or sudden transient. The selected PCM should have melting temperature below the device's maximum operating temperature, a high latent heat of fusion per unit mass, a high thermal conductivity, a high specific heat and a small volume change on phase change [1]. However, most PCMs with low melting point (such as Eicosane) also possess the undesirable property of low thermal conductivity, which results in chip overheating. This phenomenon is also known as the "self-insulating" effect of PCMs. In order to make a PCM suitable for electronics cooling applications, it becomes necessary to add some amount of high thermal conductivity material (such as aluminium or copper), which are known as thermal conductivity enhancers (TCEs).

Comprehensive descriptions of experimental and computational assessment of PCM-based thermal management for different electronic systems are presented in [2–7]. Among the studies regarding enhancement of heat transfer through PCMs using TCEs, Tong et al. [8] studied the possibility of heat transfer enhancement of a low thermal conductive PCM (water/ice system, in this case) by inserting an aluminum matrix. Humphries and Griggs [9], Witzman et al. [3] and Snyder [5] examined the effect of using flat fins for thermal enhancement. Snyder [5] modeled a finned PCM unit by using effective thermo-physical properties and neglecting melt convection. Abhat [1] performed a combined experimental and computational study of a

* Corresponding author. Tel.: +91 80 2293 3225; fax: +91 80 2360 4536.
E-mail address: pradip@mecheng.iisc.ernet.in (P. Dutta).

0017-9310/$ - see front matter © 2005 Elsevier Ltd. All rights reserved.
doi:10.1016/j.ijheatmasstransfer.2005.10.039

Nomenclature

A	coefficient in Darcy source term
a_P, a_P^0	coefficients in discretization equation
b	constant in the porosity source term
c	specific heat
C	inertia coefficient in Forchheimer's extension
d	diameter of the TCE matrix
Da	Darcy number
e	sensible enthalpy
E	enthalpy
f_s	solid fraction
f_l	liquid fraction
g	gravitational acceleration
h	heat transfer coefficient
H	height of the thermal control unit
k	thermal conductivity
K	permeability
l	length of the thermal storage unit
L	latent heat of fusion of PCM
M	morphology constant
$\dot{q}$	heat generation rate
Q	chip power
S	source term
t	time
T	temperature
u	velocity
x, y, z	coordinate axes

Greek symbols

α	thermal diffusivity
β	thermal expansion coefficient
ρ	density
ϕ	porosity of the metal matrix
μ	dynamic viscosity
ΔE	change in enthalpy
θ	dimensionless temperature
τ	dimensionless time

Subscripts

amb	atmospheric
i	tensor variable
max	maximum value
min	minimum value
melt	value at melting temperature
m	TCE
n	level of iteration
p	PCM
0	initial state
old	old iteration value
ref	reference state

thermal control unit, where PCM was incorporated in hexagonal honeycomb cells aligned parallel to the heating surface. Recently, Pal and Joshi [10] investigated melting of PCM inside honeycomb cores mounted such that the cells are vertical. Numerical simulation was performed both for a single cell and at the system level, considering the effect of natural convection in the PCM. The system level simulation results were in good agreement with the experimental data. Alawadhi and Amon [11] investigated the effectiveness of a thermal control unit (TCU) made of PCM and aluminum fins for portable electronic devices.

It may be observed from the above discussion that substantial amount of work has been reported on thermal management of electronics using PCM and metal fins. It is also apparent that there is a need for finding an effective method for heat transfer enhancement of PCMs by inserting high thermal conductivity materials. The objective of the present work is to establish a numerical model for studying the effectiveness of thermal storage units (TSUs) with PCM and TCE arrangement. The model can be suitably applied to find the optimum proportion of TCE materials for a given configuration of TSU. In this work, a generalized computational model is developed to assess the heat transfer performance of some common types of TCE distribution considering conduction heat transfer in the solid regions and natural convection heat transfer in the melted PCM. Essentially, two types of TSU's are modeled: one with the PCM distributed uniformly in a porous TCE matrix and the other with the PCM having fins of TCE material. Heat transfer enhancement with various volume fractions of TCE for different configurations is studied with respect to the variation of heat source (or chip) temperature; melt fraction and dimensionless temperature difference within the PCM, with time.

2. Mathematical model

The mathematical model is described with respect to two physical situations. For this purpose, two basic types of TCE distribution have been studied. In the first kind (Case 1), the heat sink is designed using a highly porous TCE matrix homogeneously distributed within the entire PCM. In the second kind (Case 2), the TCE is arranged in the form of fins protruding out of the base of the heat sink, while the rest of the space is filled with the PCM. For the latter arrangement, both plate-type and rod-type (pin) fins are considered. The two arrangements are shown schematically in Fig. 1. In each of the above configurations, conduction and convection (as a result of melt flow) are taken as the mode of heat transfer within the composite heat sink. Mathematical models for the two cases are outlined below.

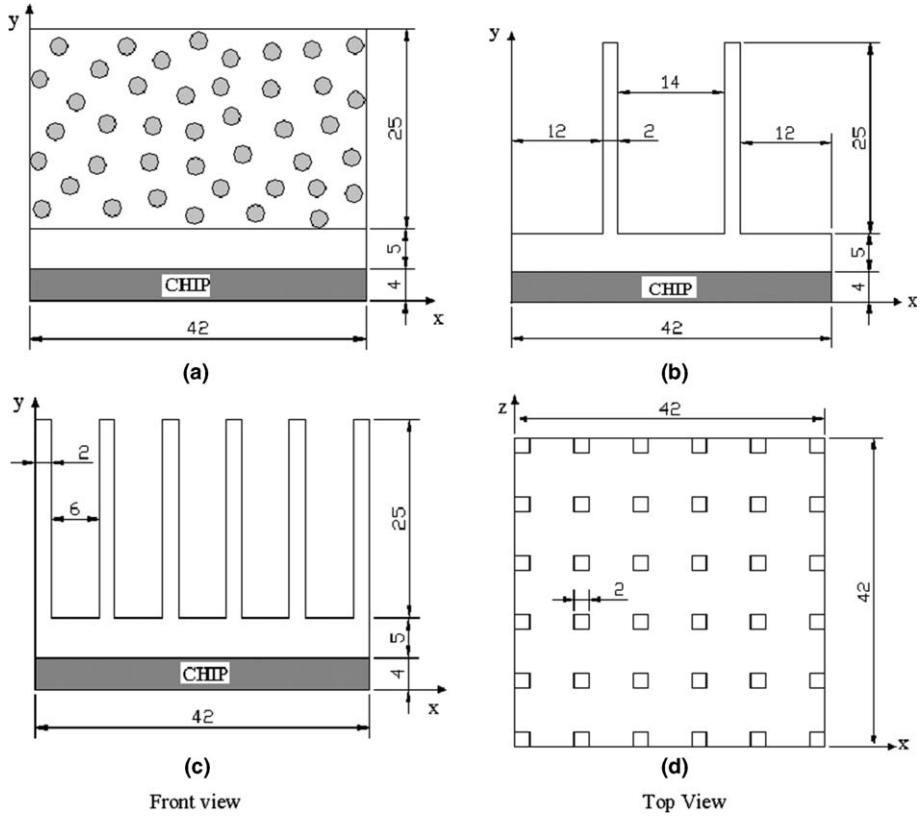

Fig. 1. Numerical models (a) matrix-type TSU, (b) plate-type TSU, (c) and (d) rod-type TSU. All dimensions are in mm.

2.1. Case 1: PCM with metal matrix (porous medium analysis)

In this case, we consider a rectangular cavity filled with a highly porous and permeable TCE (aluminum) matrix and PCM, distributed homogeneously. The thermal storage unit (consisting of PCM and TCE) is kept on an aluminum substrate, which, in turn, seats over an electronic chip or a heat source. Initially, the whole system is kept at ambient temperature, T_{amb}. The porosity of the metal matrix, ϕ_m, is assumed to be equal to the volume fraction of the PCM. The boundary conditions are such that the side and bottom faces are insulated and the top face is subjected to convective cooling. We consider constant heat generation at the heat source, which is distributed uniformly throughout the chip. This heat source (chip) requires cooling. As heating goes on, melting begins within the PCM by absorbing latent heat of fusion along with the sensible heat from the chip. But the TCE always remains in the solid state and absorbs only sensible heat. Local thermodynamic equilibrium between the PCM and the porous aluminium matrix is assumed. For the present study, Eicosane is selected as the PCM material, primarily because of its high value of latent heat of fusion. Thermo-physical properties of the homogeneous mixture of PCM and TCE matrix are calculated using a volume-averaging technique [12,13]. Because of the geometry and boundary conditions chosen, the heat transfer and fluid flow analyses in this case are assumed to be two-dimensional. Based on the volume-averaging technique, a common set of governing conservation equations for both the solid and liquid regions of the porous medium can be written as follows:

Conservation of mass

$$\frac{\partial(\rho_p u_i)}{\partial x_i} = 0 \tag{1}$$

Conservation of momentum

The equivalent singe phase momentum conservation equation for the porous medium in the ith direction is given by

$$\frac{\partial(\rho_p u_i)}{\partial t} + \frac{\partial(\rho_p u_i u_j)}{\partial x_j} = -\frac{\partial p}{\partial x_i} + \nabla\cdot(\mu\nabla u_i) + \rho_p g_i \beta(T - T_{ref}) - \left(\frac{\mu}{K} + \frac{\rho C}{\sqrt{K}}|u_i|\right)u_i \tag{2}$$

where g_i is the acceleration due to gravity in the ith direction, T_{ref} is the reference value of temperature, C is the inertia coefficient in Forchheimer's extension and K is permeability. The permeability, K, and porosity, ϕ, are correlated approximately by the Blake–Kozeny model [8], and is given by

$$K = \frac{d^2\phi^3}{175(1-\phi)^2} \tag{3}$$

where ϕ is the porosity and d is the TCE matrix diameter. The value of ϕ depends on the total solid fraction of the

medium. When the PCM is in a complete molten state, $\phi = \phi_m$, where ϕ_m is the porosity of the metal matrix. Otherwise, when the PCM is fully or partially solid, ϕ is modified according to the enthalpy porosity formulation for phase change, which is described subsequently.

The value of the inertia coefficient C has been obtained experimentally by Ward [14]. Although C is a function of the microstructure of the porous medium [15], Ward [14] found that for a large variety of porous media, it could be taken as a constant ($\sim$0.55).

The term $|u_i|$ used in Eq. (2) is defined as

$$|u_i| = \sqrt{u_1^2 + u_2^2} \tag{4}$$

In our study we have used $\frac{d}{l} \sim 10^{-2}$, where l is the length of thermal storage unit.

2.1.1. Energy conservation

The single-phase energy conservation equation for porous media is given by

$$\frac{\partial(\rho c_{\text{eff}} T)}{\partial t} + \frac{\partial(\rho c_{\text{eff}} u_i T)}{\partial x_i} = \nabla \cdot (k_{\text{eff}} \nabla T) + S_h \tag{5}$$

where ρc_{eff} and k_{eff} are the effective thermal capacitance and effective thermal conductivity, respectively, of the porous medium. The term S_h is the latent heat source term, in which the subscript 'h' represents enthalpy. The effective thermal capacitance is calculated, in the following manner, using the well known volume-averaged technique:

$$\rho c_{\text{eff}} = \rho_p c_p \phi_m + \rho_m c_m (1 - \phi_m) \tag{6}$$

The effective thermal conductivity for the porous medium is determined, in the following manner, using Veinberg model [8,16]:

$$k_{\text{eff}} + \left(\frac{k_{\text{eff}}}{k_p}\right)^{1/3} (k_m - k_p)\phi_m - k_m = 0 \tag{7}$$

where k_m is the thermal conductivity of TCE matrix and k_p is the thermal conductivity of the PCM.

2.1.2. Enthalpy–porosity formulation for phase change

In this model, we use a single domain enthalpy–porosity technique (appropriately modified) for modeling phase change and fluid flow in the porous medium. The advantage of this model is that no explicit velocity or thermal conditions are to be satisfied at the solid liquid interface. A detailed description of this approach is available in [17]. Essentially, in this approach, the solid–liquid interface in a phase change process is assumed to be a mushy region, which is approximated as a porous medium whose porosity is a direct function of the local liquid fraction. In the momentum conservation equations, a flow resistance source term as a function of porosity (and hence of solid fraction) is included. This source term ensures zero velocity in the fully solid region and permits normal viscous liquid flow in the fully liquid region. For phase change of a pure substance, however, the sharp solid–liquid interface is represented by a numerical mushy region having a thickness of only one control volume, across which there is a smooth variation of velocity and thermo-physical properties. It may be recognized here that flow in a pure substance phase change process can be modeled alternatively by an effective viscosity method. The present method, however, offers the added advantage of straightforward extension to binary mixtures, which undergo phase change within a range of temperatures.

The enthalpy formulation for the porous media energy equation (5) leads to the latent heat source term, S_h, which is given by

$$S_h = -\frac{\partial}{\partial t}(\rho \Delta E) \tag{8}$$

where

$$\begin{aligned} \Delta E &= 0, \quad T < T_{\text{melt}} \\ &= \phi_m L, \quad T > T_{\text{melt}} \end{aligned} \tag{9}$$

where T_{melt} is the melting temperature of PCM, and L is its latent heat of fusion.

It is important to note that the latent enthalpy content of the control volume in the porous medium is $\phi_m L$ after melting. This is so because a fixed volume fraction $(1 - \phi_m)$ of TCE matrix is always present, which absorbs only sensible heat. This enthalpy value is to be accurately updated in every iteration within a particular time step. Since the chip and substrate absorb only sensible heat, ΔE for these regions should be set to zero.

Referring to the expression for permeability given in Eq. (3), it may be noted that for the molten control volumes, liquid fraction is ϕ_m, while for fully solid zones this is equal to zero. Hence, the solid region permeability should ideally become zero. In order to model this effect, the effective porosity of the TCE matrix is decreased, depending on the solid fraction of the PCM. The solid fraction, f_s, of the PCM can be expressed as

$$f_s = 1 - (\text{liquid fraction of PCM}) = 1 - \frac{\Delta E}{\phi_m L} \tag{10}$$

Table 1
Thermo-physical properties of the PCM used

Eicosane	Density (kg/m^3)	Kinematic viscosity (m^2/s)	Thermal conductivity (W/m K)	Specific heat (J/kg K)	Melting point (°C)	Latent heat (J/kg)	β (1/K)
Solid	810		0.39	1900			
Liquid	770	4.5e−6	0.157	2200			
Value used	790	4.5e−6	0.23	2050	37	241,000	10^{-3}

Table 2
Thermo-physical properties of TCE (or substrate) and chip used

	Density (kg/m^3)	Thermal conductivity (W/m K)	Specific heat (J/kg K)
TCE/substrate	2712.9	179.6	960
Chip	740	20	1830

Hence, the effective porosity of the medium can be expressed as

$$\phi = \phi_m - \left(1 - \frac{\Delta E}{\phi_m L}\right)\phi_m = \phi_m - (1 - f_s)\phi_m \tag{11}$$

As a consequence of this, the coefficient of the source term in Eq. (3) becomes very large when the PCM is in

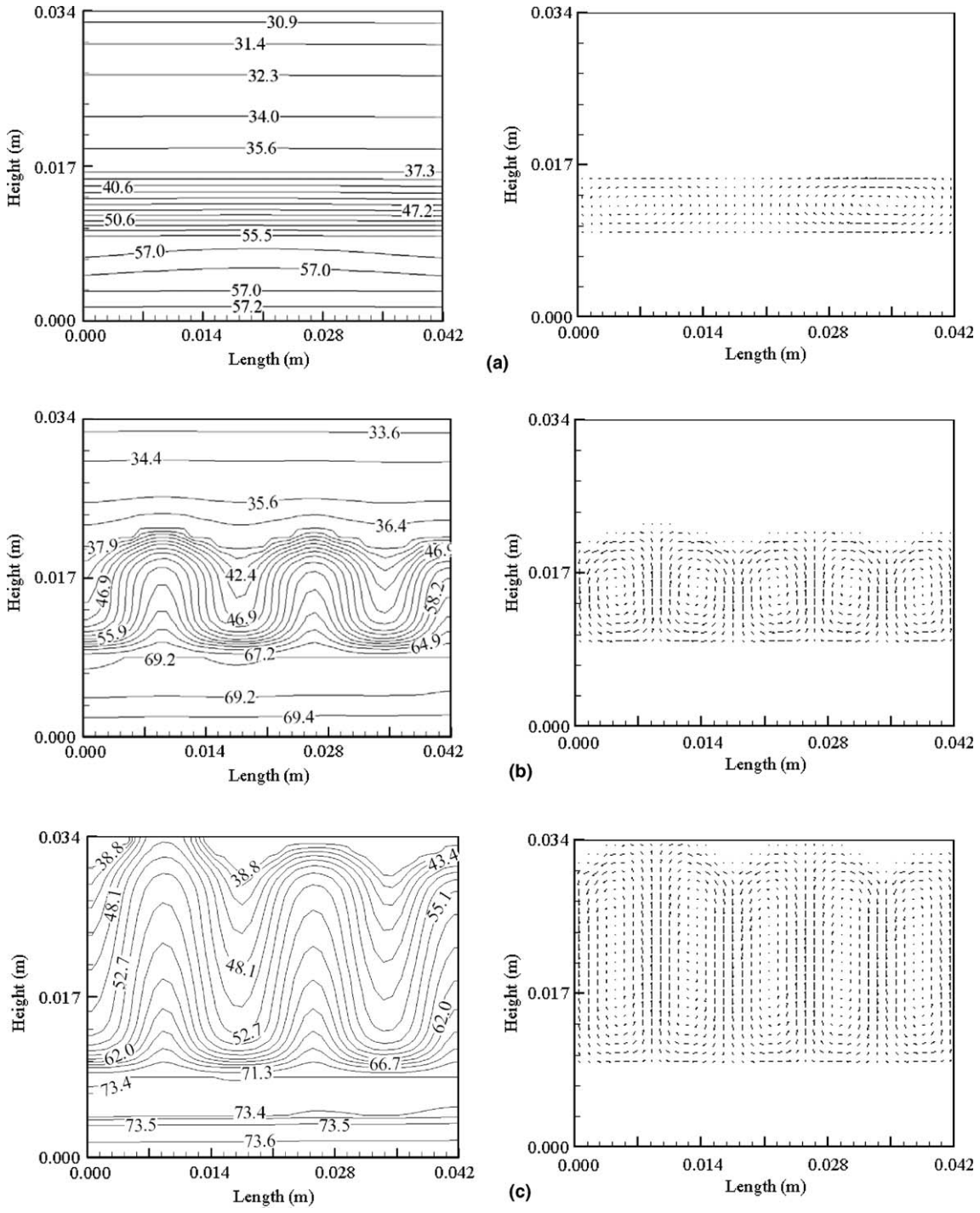

Fig. 2. Temperature and velocity field evolution of PCM melting with TCE matrix ($\phi = 0.85$, $Da = 4.74 \times 10^{-5}$): (a) 2100 s; (b) 2700 s and (c) 3600 s at 4 W. U_{max} in above cases are (a) 3×10^{-6} m/s; (b) 2.98×10^{-4} m/s; (c) 2.73×10^{-4} m/s.

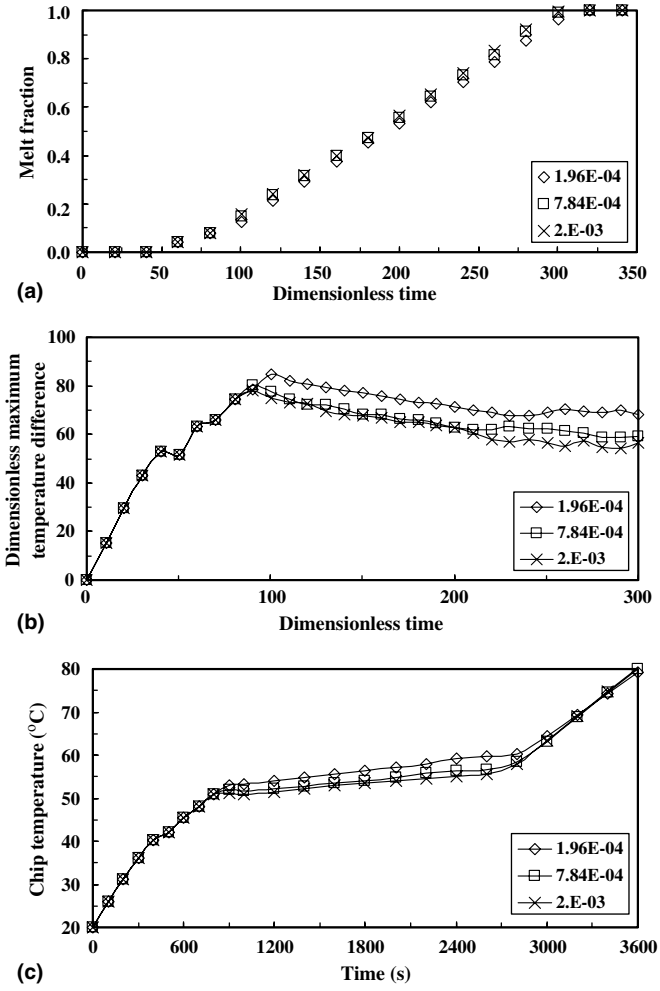

Fig. 3. Effect of Darcy number (Da) on (a) melt fraction, (b) uniformity and (c) chip temperature at 4 W.

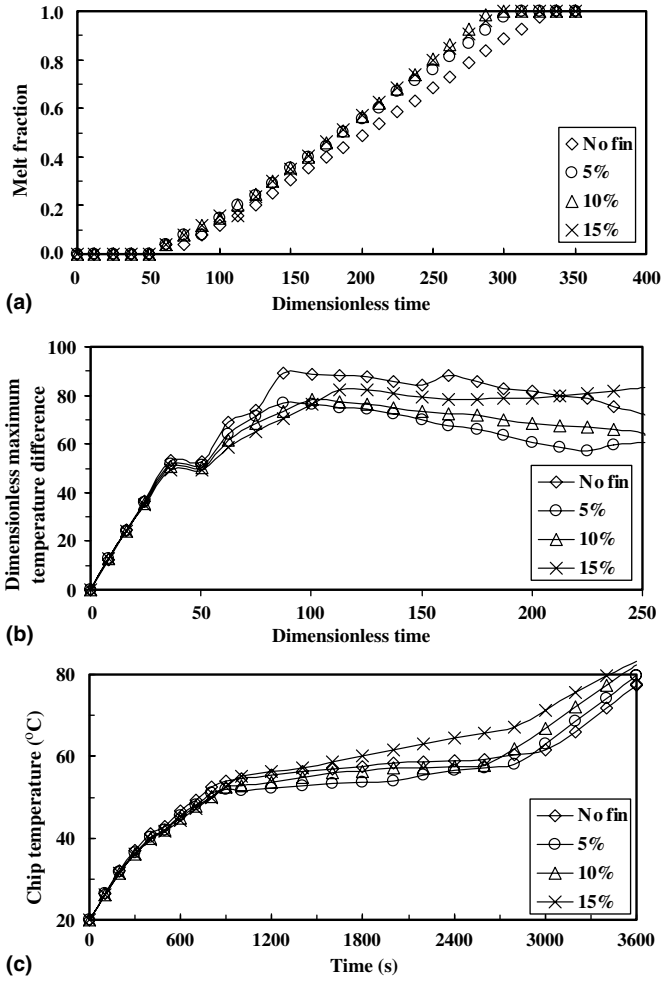

Fig. 4. Effect of TCE matrix amount on (a) melt fraction, (b) uniformity and (c) chip temperature (for $d/l = 2 \times 10^{-2}$) at 4 W.

the solid state. This will swamp out all terms in the governing momentum equations and force any velocity predictions in the solid region effectively to zero. In the liquid region ϕ value depends on the volume fraction of TCE matrix and is always less than one. Hence, the source term does not vanish even in the molten region. This induces drag to the fluid flow. Its magnitude depends on permeability K, ρ_p, μ and fluid velocity. As the magnitude of the source term increases, the effect of convection diminishes. At this point conduction becomes the dominating mode of heat transfer. It may be noted here that the chip and substrate are also included in the domain, by treating them as fully solid materials. To ensure zero velocity in the chip and substrate, a high value of viscosity ($\sim 10^{20}$ m^2/s) is assigned for these regions. Additionally, a heat source term $\dot{q}$ is included for the heater region.

2.2. Case 2: PCM with TCE fins

In Case 2, the thermal storage unit is filled with PCM and TCE fins with a given volume fraction of fin material. The rest of the configuration and the boundary conditions are similar to those of Case 1. However, because of the structured geometry of the arrangement, this case can be modeled using separate thermo-physical properties of the two substances. Hence, in this case, determination of effective thermo-physical properties for the thermal storage unit is not required.

Two types of configurations are considered for Case 2. The first type (Case 2a) deals with plate-type fins oriented in a particular direction. For this case, neglecting end effects, lengthwise variations of temperature and fluid flow can be ignored. Hence, the heat transfer and fluid flow analyses for this situation are based on a two-dimensional approach. For the second configuration (Case 2b), the thermal storage unit is filled with PCM and rod-type TCE fins. The rest of the arrangement is similar to that of Case 2a. Since the fins in this case are of rod-type, the heat transfer and fluid flow cannot be analyzed using a two-dimensional approach. Hence, a three-dimensional study is carried out for this case.

The governing equations are written following a single domain approach, as in Case 1. However, in absence of the porous TCE matrix, ϕ_m in the present case is equal

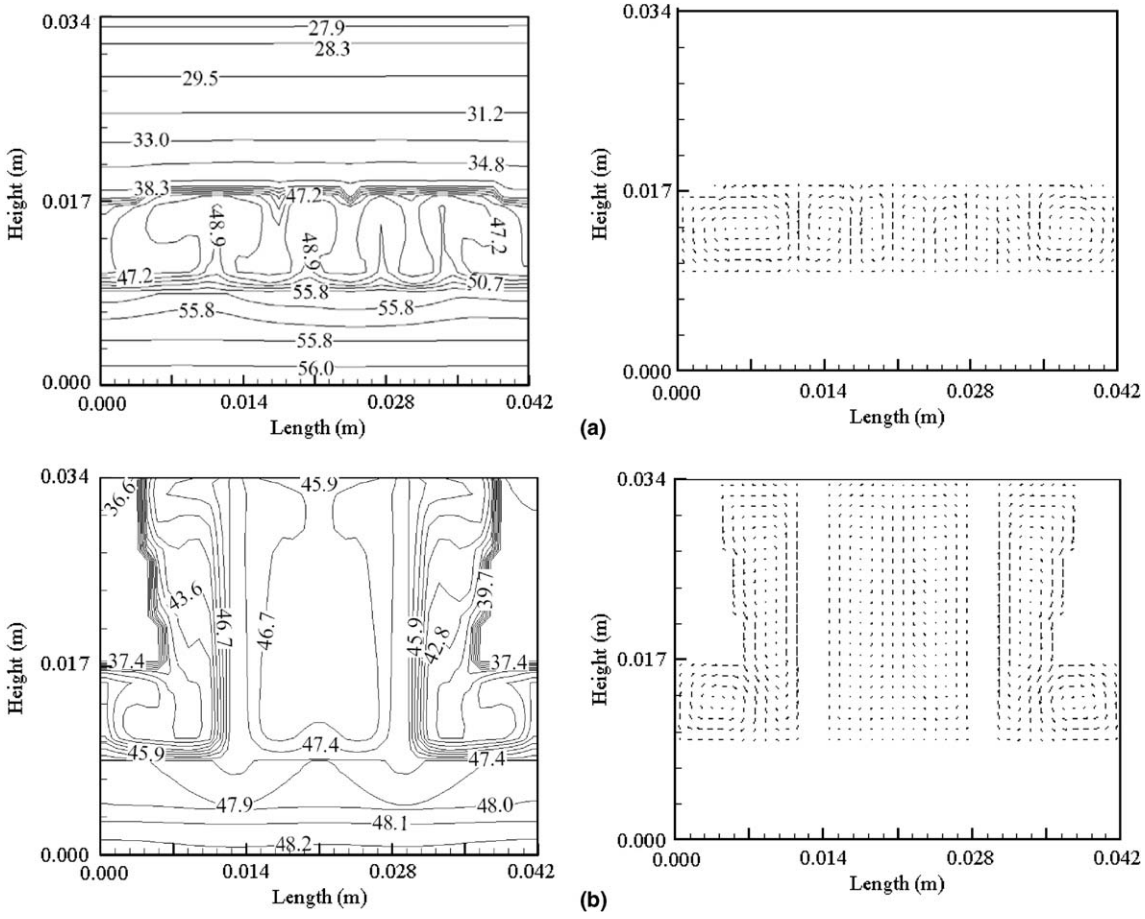

Fig. 5. Isotherms and velocity vectors for a power level of 4 W with (a) no fin and (b) 10% volume fraction of TCE; time = 2400 s.

to one. The TCE, chip and substrate materials are assigned very high viscosity ($\sim 10^{20}$ m^2/s) and melting point, which ensures that they remain solid and fixed in the domain. The rest of the formulation and analysis are same as that of Case 1, and are not repeated here.

2.3. Updating nodal heat content

An accurate prediction of the liquid fraction in the fixed-grid enthalpy-based procedure used here, it is necessary to update the latent heat content of each computational cell. This is done in conjunction with temperature values predicted by the macroscopic conservation equations, during each iteration within a time-step. In the present case, to update the nodal latent heat content of a computational cell at Pth node point, an iterative updating scheme proposed in [17] is preferred. This has the following form:

$$[\Delta E_P]^{n+1} = [\Delta E_P]^n + \frac{a_P}{a_P^0}\lambda\left[\{e_P\}^n - cF^{-1}\{\Delta E_P\}^n\right] \tag{12}$$

where ΔE_P is the latent heat content of the computational cell, n is the iteration number, $a_P^0 = \rho\Delta V/\Delta t$, a_P is the coefficient of T_P in the discretization equation of the governing energy equation, λ is the relaxation factor (set to 0.1 in this study), e is the sensible enthalpy, c is the specific heat, F^{-1} is the inverse latent heat function, ΔV is the volume of the computational cell centered around the grid point P, Δt is the time step chosen. The physical meaning of the term a_P/a_P^0 is described in [17]. Since the PCM used in the present study is considered to be a pure substance, F^{-1} will be equal to cT_{melt}.

2.4. Initial and boundary conditions

As the initial state and boundary conditions are similar in both Case 1 and Case 2, a common set of appropriate initial and boundary conditions are adopted.

The initial conditions appropriate to the physical situation are:

At $t = 0$, $T = T_0$, $f_l = 0$.

The boundary conditions adopted for solutions of conservation equations are:

1. No slip condition at the walls, i.e. $u = v = w = 0$.
2. Natural convection with the ambient at the top, i.e. $-k\frac{\partial T}{\partial x}\big|_{y=H} = h(T|_{y=H} - T_{\text{amb}})$.
3. Insulated side walls and bottom; i.e. $\frac{\partial T}{\partial x}\big|_{x=0,L} = 0$ along vertical walls and $\left.\frac{\partial T}{\partial y}\right|_{y=0} = 0$ for bottom.

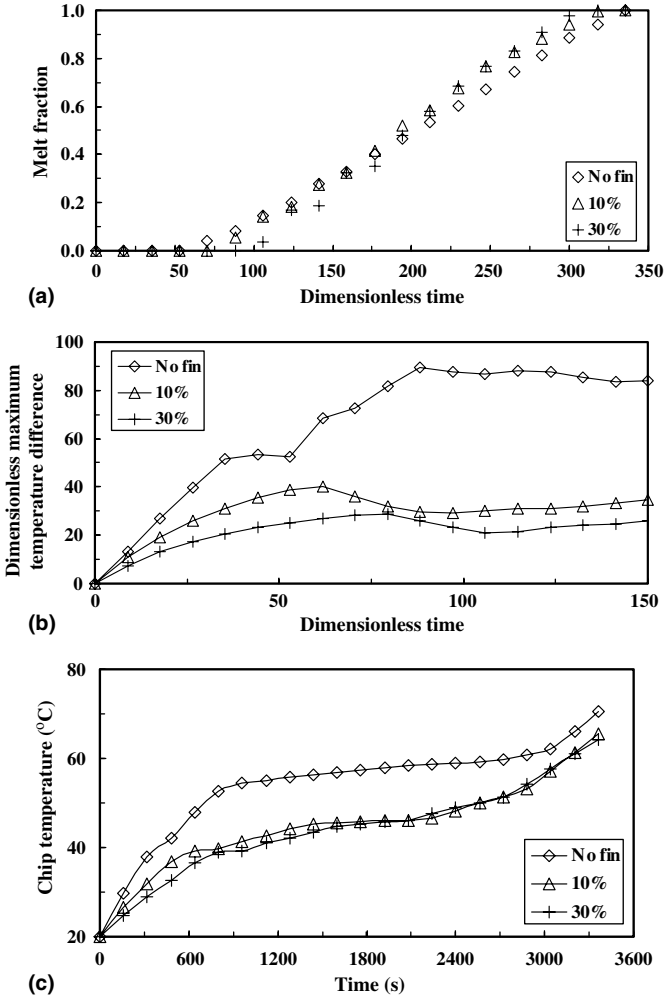

Fig. 6. Timewise variation of (a) melt fraction, (b) maximum temperature difference within the PCM and (c) chip temperature for various TCE volume fractions at 4 W.

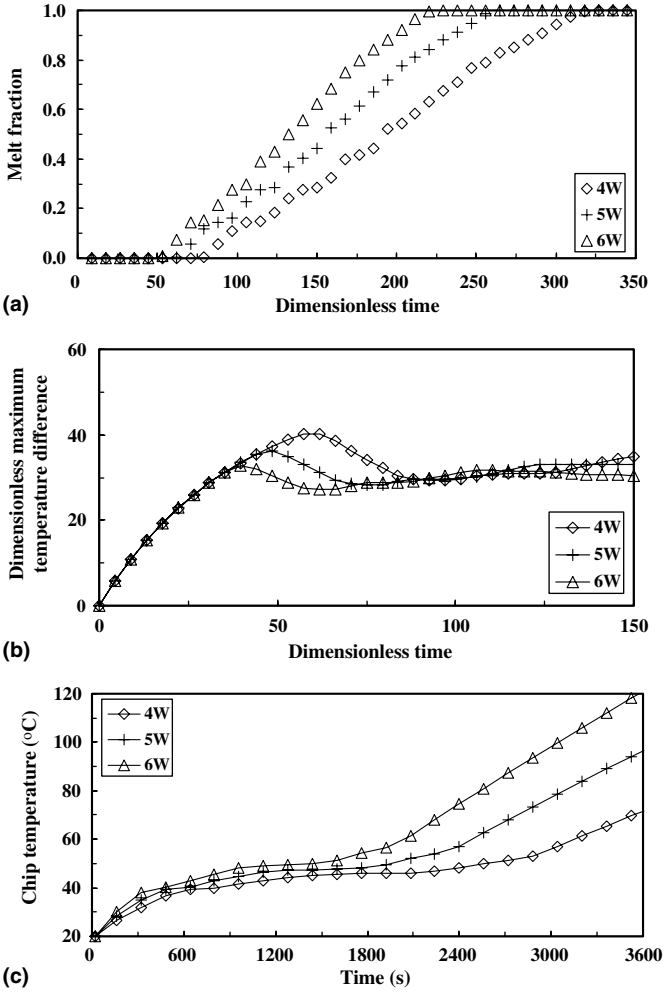

Fig. 8. Timewise variation of (a) melt fraction, (b) maximum temperature difference within the PCM and (c) chip temperature at different chip power level for 10% volume fraction of TCE.

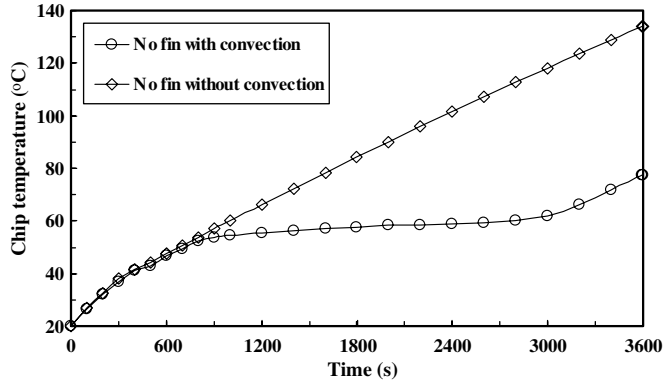

Fig. 7. Effect of melt convection on heater temperature at 4 W.

3. Results and discussion

The governing equations described in the previous section are solved iteratively using a pressure based finite volume method according to the SIMPLER algorithm [18]. Numerical simulations are performed for both the cases, namely PCM with TCE matrix (Case 1) and PCM with TCE fins (Case 2). The dimensions of heat sinks used for the case studies are given in Fig. 1. Since the top surface is cooled by natural convection, a nominal value of $h = 10\ \mathrm{W/m^2\,K}$ is used. It is also observed that the results are not sensitive to the value of h during the melting stage as most of the heat released from the chip is absorbed in the TSU as latent heat. A comprehensive grid-independence study is undertaken to determine the appropriate spatial discretization, temporal discretization and iteration convergence criteria to be used. The quantities examined in this study are maximum magnitudes of various scalar variables (i.e. components of velocity and temperature). As an outcome of this study, we have taken a $42 \times 34 \times 42$ uniform grid in 3-D, and 42×34 uniform grid in 2-D as our final simulation matrix. Also, the time steps are kept high (2 s) at the initial stages of simulation in the conduction regime. Once the melting starts the time step is reduced to 0.2 s for better convergence. Time steps may be increased after melting is sufficiently developed.

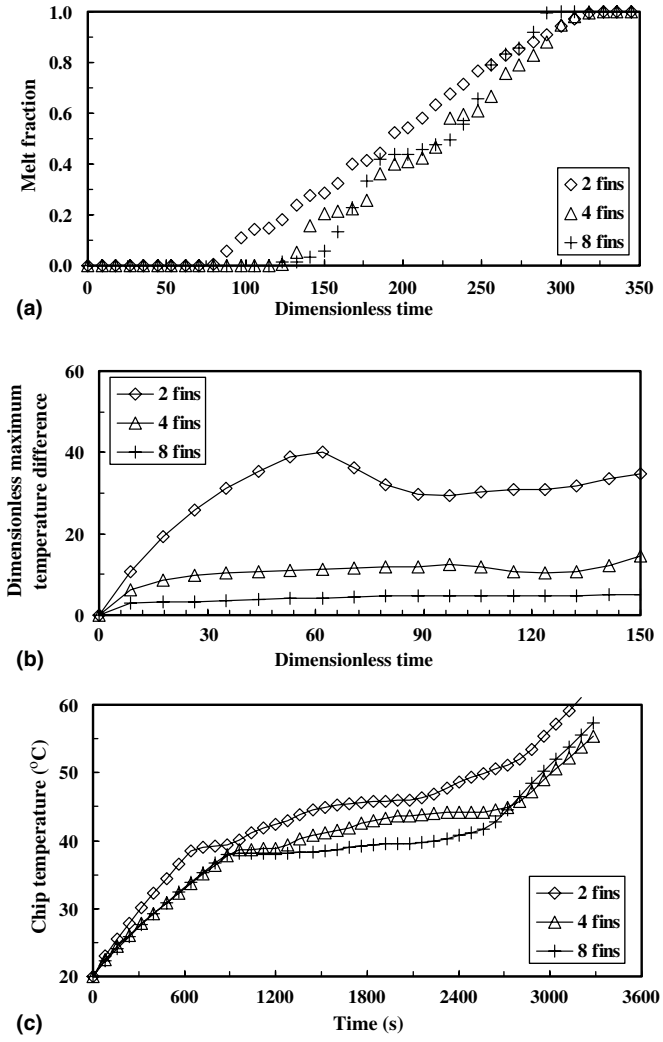

Fig. 9. Timewise variation of (a) melt fraction; (b) dimensionless maximum temperature difference within the PCM and (c) chip temperature for different fin distribution at 20% volume fraction of TCE and 5 W.

The results are studied with the help of an appropriate set of dimensionless parameters, which are defined as follows:

Dimensionless time: It is given by

$$\tau = \frac{\alpha_m t}{l^2} \tag{13}$$

where α_m is the thermal diffusivity of TCE, l is length of the thermal storage unit, and t is time.

Dimensionless maximum temperature difference within the thermal storage unit: It is defined as

$$\theta_{max} = (k_m l^2/QH)(T_{max} - T_{min}) \tag{14}$$

where k_m is the thermal conductivity of the TCE, H is the height of the thermal storage unit, Q is the chip level power, T_{max} is the maximum temperature and T_{min} is the minimum temperature, respectively, within the thermal storage unit. θ_{max} gives an idea about the range of temperature variation within the PCM. A lower value of θ_{max} implies less inclination for overheating. It also ensures uniform melting and stabilized chip temperature.

Darcy number: This number is relevant only in Case 1, and is defined as

$$Da = K/l^2 \tag{15}$$

where K is the permeability of the porous media.

3.1. Results for PCM with porous metal matrix (Case 1)

The simulations are based on the physical properties of solid PCM, liquid PCM and the aluminum matrix, as given in Tables 1 and 2. The effective thermal conductivity of the porous medium is determined according to the Veinberg model described in [16].

Fig. 2 shows the evaluation of flow and temperature fields, for the case of heating of PCM with TCE. It is observed that the heating process is initially dominated by conduction. Once melting begins, convection sets in and enhances the heat transfer rate from the base of the heat sink. Rayleigh–Benard convection cells are formed in the molten PCM as the molten layer is heated from below, leading to a wavy liquid–solid interface. Similar simulations are performed with various values of the Darcy number (Da) and the effect of convection is studied. It is observed that the effect of convection is more pronounced at high Da, implying that a metal matrix insert enhances conduction and inhibits convection. The heat transfer mechanism changes from a conduction regime to a conduction–convection regime, as Da is increased. If Da is reduced by decreasing the size of the spherical matrix, conduction becomes the dominant mode of heat transfer. It is shown in Fig. 3 that a reduction of Da from 2.0×10^{-3} to 1.96×10^{-4} results in lower melting rate, higher chip temperature and less uniformity of temperature within the PCM. When the Darcy number is high, there is less resistance to convective fluid motion in the molten PCM layer. A stronger melt convection results in quicker heat transfer from the base plate to the upper regions of the heat sink, resulting in an increased PCM melting rate. Hence, one can conclude that for the same volume fraction of TCE matrix, the cooling performance is better for a larger matrix size.

Fig. 4 shows the effect of TCE volume fraction on various quantities such as melt fraction, uniformity of temperature in PCM and chip temperature. It is observed that the melting duration is reduced by inserting a TCE matrix. It may be noted that the enhancement of melting is large at low volume fractions of the TCE matrix (~5%). Subsequent increase in volume fraction does not increase melting rate linearly (Fig. 4(a)). This is expected because at higher volume fractions of the metal matrix, the metal network provides more resistance to melt flow, resulting in a conduction dominated heat transfer. One can note from Fig. 4(a) that the melting duration for 15% of TCE volume fraction is higher than that for 10% of TCE volume fraction. This occurs because the conduction dominated heat transfer delays melting of PCM.

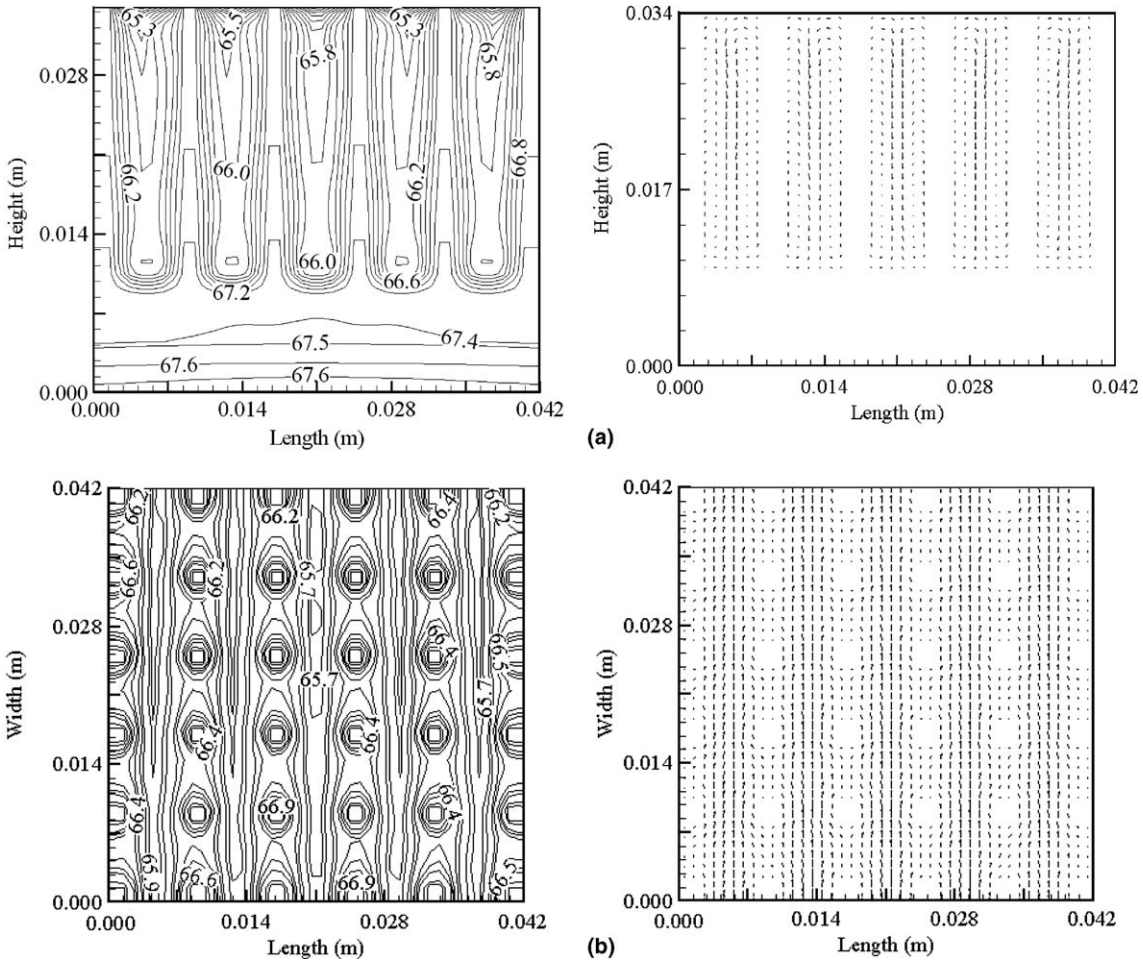

Fig. 10. Isotherms and velocity vectors for the system with rod-type aluminum fins at (a) $z = 0.018$ m, (b) $y = 0.034$ m for chip power of 4 W and time = 3900 s.

It is also observed that uniformity of temperature within the PCM is better at a low volume fraction (~5%) of TCE. With a high TCE volume fraction, the effect of convection diminishes, resulting in non-uniformity of temperature within the PCM (Fig. 4(b)). Also, the chip temperature is found to be lower for a smaller volume fraction of TCE. With a high volume fraction of TCE, heat transfer is primarily by conduction (enhanced by TCE), resulting in a thermal stratification within the TSU. Consequently, the chip temperature will be higher. One can note that even at 15% volume fraction of TCE, chip temperature is higher than that of the base case.

3.2. Results for PCM with metallic fins (Case 2)

In this case, computation is carried out with Eicosane as the PCM and with the TCEs arranged in the form of plates or rods (or pin fins) as shown in Fig. 1. First, the two-dimensional case of plate-type fins is considered. The property values used in the computation are listed in Tables 1 and 2. The thermo-physical properties of the PCM and TCE are assumed to remain constant within the operating temperature range. The effects of various parameters on the thermal performance of the system are discussed. Finally, the thermal performances of heat sinks with plate-type and rod-type fins are compared for a given set of parameters.

Fig. 5 shows the temperature and velocity fields within the TSU after 2400 s of heating with a chip power level of 4 W, for the case of plate fin arrangement. Fig. 5(b) show a significant advantage of adding plate-type TCE fins in comparison to the baseline case (Fig. 5(a)). Because of low thermal conductivity of the PCM, heat from the chip is not easily dissipated. Hence, the chip temperature rises within a short time interval, leading to local overheating of the PCM adjacent to the chip. But when certain amount of TCE is added, the effective conductance is significantly increased. The TCE fins absorb heat at a faster rate and diffuse it away from the base. Hence, melting of the PCM is initiated at multiple locations, at the base as well as along the fins. Accordingly, convection cells are formed within the molten PCM, as shown in Fig. 5(b).

It is observed from Fig. 6(b) and (c) that a 10% volume fraction of TCE gives temperature uniformity and chip temperature which is comparable to that with 30% TCE. However, higher TCE volume fraction implies less latent heat storage. Hence, an optimum TCE volume fraction

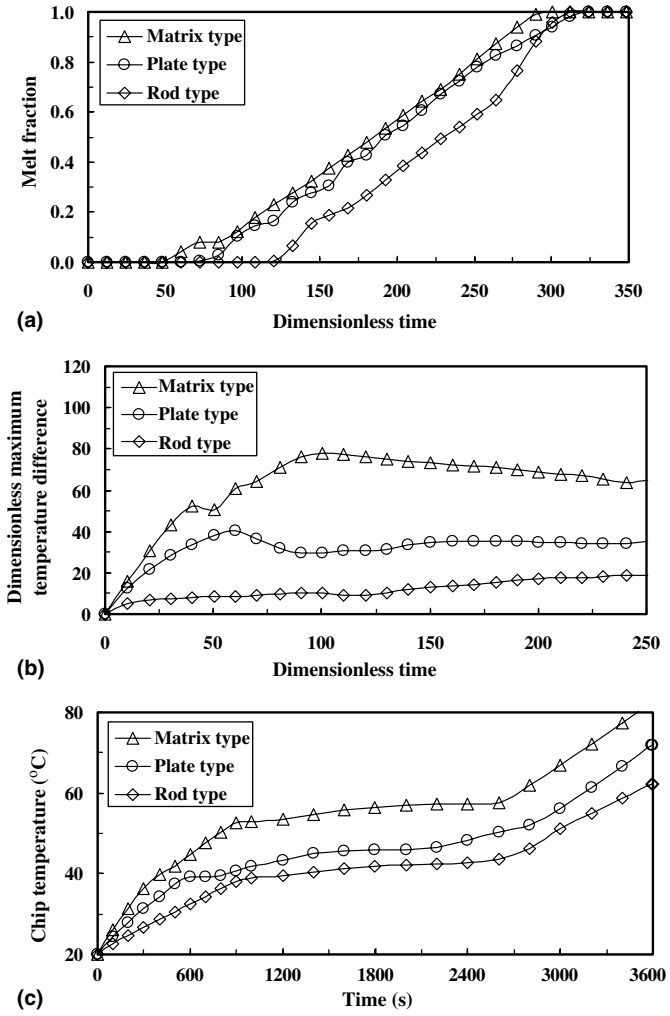

Fig. 11. Comparative study of thermal performance of TSUs having TCE of matrix-type; plate-type and rod-type at 4 W.

of about 10% can give an ideal heat sink performance from the point of view of chip temperature and latent heat storage.

In order to bring out the effect of natural convection within the melt region, the variation of chip temperature with time is plotted for the cases with and without melt convection (Fig. 7). Natural convection of molten PCM promotes good mixing and reduces thermal stratification within the melt. Hence, it enhances the melting rate of solid PCM while maintaining temperature uniformity within the liquid phase. This stabilizes the chip temperature close to the PCM melting temperature. Hence, the effect of natural convection of the molten PCM cannot be ignored for the present arrangement.

The results for effect of chip power on various quantities of interest are shown in Fig. 8. As expected, melting duration reduces with increase of chip power. Hence, if one needs to operate the equipment at a high chip power level, more quantity of PCM or a PCM with a high latent heat will be required. Fig. 8(b) demonstrates that power level does not affect non-dimensional temperature field within the PCM significantly. The reason is that the rate of temperature gradient and power level depends mainly on the thermal conductivity of the TSU material. At a high chip power level, the temperature of the system as a whole may rise, but the non-dimensional temperature difference between any two points in the system does not alter much. The chip temperature, however, rises faster with higher chip power until melting is initiated (Fig. 8(c)).

The effect of fin number (or fin thickness) is also studied, for a particular TCE volume fraction, TCE material, and chip power level. Studies are conducted by distributing 20% of TCE volume fraction in 2, 4 and 8 fins, and the results are shown in Fig. 9. It is observed that the larger the number of fins, the more is the temperature uniformity. The increase in temperature uniformity is caused by the higher thermal diffusivity of the TCE material. With more TCE fins distributed throughout the heat sink, the heat from the base plate diffuses quickly, thus delaying local overheating near the base plate. Hence the PCM adjacent to the base plate reaches the melting temperature at a later time. Although the onset of PCM melting is delayed with more TCE fins, the melting process is initiated at several locations and the entire PCM melts in a shorter time (Fig. 9(b)).

Computations are also performed for the case of PCM with rod-type TCE fins. For this case, a three-dimensional conjugate heat transfer study is necessary, as discussed earlier. Fig. 10 shows the velocity and temperature fields of the system along two different cross-sectional planes. Fig. 10(a) shows circular isotherms around each rod fin. From Fig. 10(b), one can note that the temperature is nearly uniform in the entire domain.

Finally, a comparative study is performed with regard to the thermal performance of the three PCM-TCE arrangements (Fig. 11). It is observed that the rod-finned arrangement maintains best uniformity of temperature in the system and keeps the chip temperature lowest. Fig. 11(a) reveals that the onset of melting is significantly delayed in the case of PCM with rod-type TCE fins, even in comparison to the case of plate-type fins. This phenomenon can be attributed to an efficient three-dimensional heat diffusion in this case, leading to slower temperature rise. However, once melting begins, the process is completed in a short time.

4. Conclusions

In the present work, some basic studies are carried out to model the thermal performance of heat sinks with phase change materials and thermal conductivity enhancers. Three types of TCEs are studied, namely porous matrix, plate-type fins and rod-type fins. A generalized enthalpy based mathematical formulation and numerical model is developed for all the cases. This enthalpy–porosity based model can be easily extended to analyze the performance of PCMs, which are mixtures or binary substances.

For the case of PCM with porous TCE matrix, it is found that inserting aluminum matrix into Eicosane can

offer an order-of-magnitude increase in thermal conductivity and melting rate. The effect of melt convection is significant at high permeability and Rayleigh number. Melt convection has a considerable effect on the evolution of the solid–liquid interface. However, the effect of convection becomes insignificant beyond a certain volume fraction of TCE. For the case of PCM with TCE fins, too, convection in the melt plays a significant role in temperature uniformity. The performance of the heat sink improves if the TCE material is distributed in the form of thinner fins. It is also found that rod-type fins perform better than plate-type ones, as they are able to maintain better uniformity of temperature within the PCM leading to less chip temperature.

Acknowledgement

The work reported in this paper is supported by a research grant from the Defence Research and Development Organisation, Government of India.

References

[1] A. Abhat, Experimental investigation and analysis of a honeycomb-packed phase change material device, AIAA Paper 1976, pp. 76–437.
[2] E.W. Bentilla, K.F. Sterrett, L.E. Karre, Research and development study on thermal control by use of fusible materials, Northrop Space Laboratories, Control No. NAS 8-11163, NASA Document No. N66-26691, 1966.
[3] S. Witzman, A. Shitzer, Y. Zvirin, Simplified calculation procedure of a latent heat reservoir for stabilizing the temperature of electronic devices, in: S. Oktay et al. (Eds.), Proceedings of the Winter Annual Meeting of the ASME, Boston, MA, HTD, 1983, vol. 28, pp 29–34.
[4] R. Chebi, P.A. Rice, J.A. Schwarz, Heat dissipation in microelectronic systems using phase change materials with natural convection, Chem. Eng. Commun. 69 (1988) 1–12.
[5] K.W. Snyder, An investigation of using a phase change material to improve the heat transfer in a small electronic module for an airborne radar application, in: Proceeding of the International Electronics Packaging Conference, San Diego, CA, 1991, vol. 1, pp. 276–303.
[6] M. Ishizuka, Y. Fukuoka, Development of a new high density package cooling technique using low melting point alloys, in: Proceedings of the ASME/JSME Thermal Engineering Joint Conference 1991, vol. 2, pp. 375–380.
[7] D. Pal, Y.K. Joshi, Application of phase change materials to thermal control of electronics modules: a computational study, Trans. ASME, J. Electron. Packag. 119 (March) (1997).
[8] X. Tong, J.A. Khan, M.R. Amin, Enhancement of heat transfer by inserting a metal matrix into a phase change material, Numer. Heat Transfer, Part A 30 (1996) 125–141.
[9] W.R. Humphries, E.I. Griggs, A design handbook for phase change thermal control and energy storage devices, NASA T.P. 1074, 1977.
[10] D. Pal, Y.K. Joshi, Thermal management of an avionics module using solid–liquid phase materials, J. Thermophys. Heat Transfer 12 (2) (1998).
[11] E.M. Alawadhi, C.H. Amon, Thermal analysis of a PCM thermal control unit for portable electronics devices: experimental and numerical analysis, in: Eight Intersociety Conference on Thermal and Thermomechanical Phenomena in Electronic Systems, San Diego, California, May 29–June 1, 2002.
[12] C. Beckermann, R. Viskanta, Natural convection solid/liquid phase change in porous medium, Int. J. Heat Mass Transfer 31 (1988) 35–46.
[13] D.N. Nield, A. Bejan, Convection in Porous Media, second ed., Springer-Verlag, New York, 1999.
[14] J.C. Ward, Turbulent flow in Porous Media, J. Hydraul. Div. ASCE 90 (HY5) (1964) 1–12.
[15] C. Beckermann, R. Viskanta, S. Ramadhyani, A numerical study of non-Darcian natural convection in a vertical enclosure filled with a porous medium, Numer. Heat Transfer 10 (1986) 557–570.
[16] J.A. Weaver, R. Viskanta, Freezing of liquid—saturated porous media, J. Heat Transfer 108 (1986) 654–659.
[17] A.D. Brent, V.R. Voller, K.J. Reid, Enthalpy porosity technique for modeling convection–diffusion phase change: application to the melting of pure metal, Numer. Heat Transfer 13 (1988) 297–318.
[18] S.V. Patankar, Numerical Heat Transfer and Fluid Flow, Hemisphere Publications, New York, NY, 1980.